CSC 585 - Assignment 4
Deep learning to predict choices using fMRI data

Chinmai Basavaraj
University of Arizona
chinmaib@email.arizona.edu

Abstract

Decision making is a process of steps that involves- information gathering, analysis, conflict resolution, and selection. We use deep learning to model the process of decision making involving risk and predict the choices using fMRI data. Prior work indicates that consumers vary in their risk preferences for experiences vs monetary gambles. They are risk-seeking for positive experiences and risk-averse for positive gains (money). We expect that consumers use extreme reference points for choices of experiences (best or worst experiences they had), which is captured by the fMRI data due to increased activity in the decision makers explicit memory of facts and events. We compare the results of a Support Vector Machine (SVM) with a Bi-directional LSTM in predicting choices. We also notice a significant improvement in choice prediction by employing an LSTM-CRF which captures the dependencies between labels.

1 Introduction

Functional magnetic resonance imaging is a non-invasive technique that measures brain activity by detecting changes associated with blood flow. The primary form of fMRI uses the blood-oxygen-level dependent (BOLD) contrast. Studying and understanding the brain functionality has proved to be beneficial for disease prevention and detection, psychological treatment and behavioral understanding. Our research is directed at expanding the extant marketing knowledge to study how consumers process product and service experiences and predict choices.

Decision making is a process of steps that involves- information gathering, analysis, conflict resolution, and selection. We use deep learning to model the process of decision making under risk and predict the choices using fMRI data.

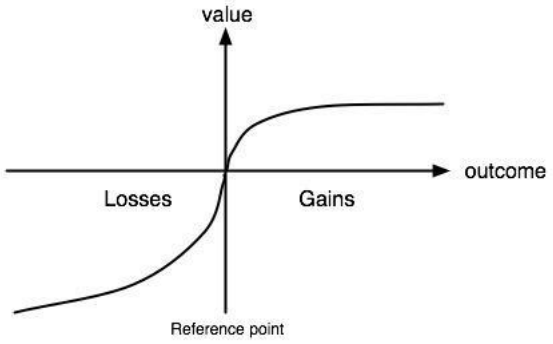

Figure 1: The value function that passes through the reference point is s-shaped and asymmetrical. The value function is steeper for losses than gains indicating that losses outweigh gains.

A wide array of research devoted to risk preferences for money exists, revealing that consumers are risk-seeking when choosing between monetary losses and risk-averse when choosing between monetary gains (Kahneman and Tversky, 1979, 1992; Rabin and Thaler, 2001). Tversky and Kahneman proposed that losses cause greater emotional impact on an individual than does an equivalent amount of gain, so given choices presented two ways with both offering the same result an individual will pick the option offering perceived gains (Figure 1). For example, most consumers will take a 50/50 chance of losing either $100 or $500 over a sure loss of $300 but choose a sure gain of $300 over a 50/50 chance of gaining either $100 or $500.

Conversely, research shows that consumers are generally risk-seeking for positive experiences and risk-averse for negative experiences, the mirror image of choices for money (Martin et al., 2016). While rating experiences, individual's extreme-best or worst experiences serve as the reference point. If our hypothesis that reference points

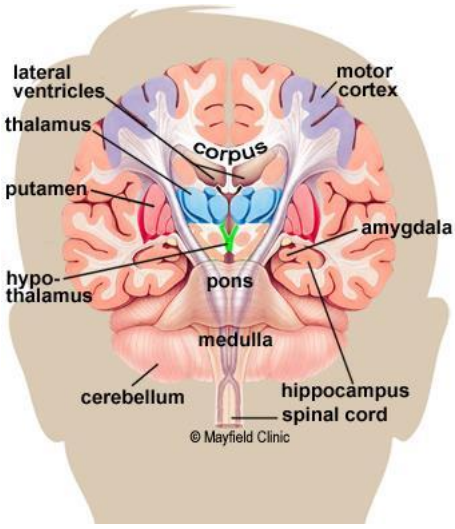

Figure 2: Coronal cross section of the human brain shows the location of the Hippocampus and the Amygdala. Hippocampus is where episodic memories are formed and indexed for later access. Amygdala attaches emotional significance to memories.

for experiences are set at more extreme outcomes holds true, then we would expect to see activation in the Memory areas- medial temporal lobe (Squire and Zola-Morgan, 1991; Kandel, 2007, 2001) (particularly, the Hippocampus and the Amygdala (Figure 2) for choices on experiences (vs. money).

In our present work, we predict consumer choices using fMRI data. We subjected the fMRI data to a Support Vector Machine (Huang and Luo, 2016) as our baseline classifier and predict the choices made by the participants in response to a stimulus. We extend our approach to this problem by using deep learning methods such as Bi-Directional LSTM (Dhruv et al., 2016). We also notice a significant improvement in choice prediction by employing an LSTM-CRF which captures the dependencies between labels.(Lample et al., 2016)

2 Related Work

In the present work, we are curious to know whether consumers access extreme reference points in memory in order to make choices on experiences (vs. money). Neurophysiologically, consumers have the ability to acquire new ideas from experiences and to retain these ideas in memory(Kandel, 2007).

Traditionally, fMRI analysis methods have focused on characterizing the relationship between cognitive variables and individual brain voxels. However, there are limits on what can be learned about cognitive states by examining voxels in isolation. Instead of focusing on individual voxels researchers use powerful pattern-classification algorithms, applied to multi-voxel patterns of activity (Kenneth et al., 2006), to decode the information that is represented in that pattern of activity. We call this approach multi-voxel pattern analysis (MVPA). The primary advantage of MVPA methods over individual-voxel-based methods is increased sensitivity.

MVPA has been used to predict the time course of recall behavior in a free-recall task (Polyn et al., 2005), and it has also been used to predict second-by-second changes in perceived stimulus dominance during a binocular rivalry task (Haynes and Rees, 2005). MVPA must be preceded by a feature selection step, which is not needed for deep learning methods. What differentiates neural networks from other classifiers, is the automatic feature learning from data which largely contributes to improvements in accuracy (Suhaimi et al., 2015).

3 fMRI Data Structure

fMRI data consisting of a time series of 441 volumes with 33 slices in the transverse plane were obtained using single shot gradient-echo planar imaging (TR = 1,000ms, TE = 30ms, flip angle = 90, resolution = 2.5mm 2.5mm 2.5mm, and FOV = 240mm). All neuroimaging data were preprocessed and analyzed using the BrainVoyager QX 20.6 analyses software (Rainer et al., 2006).

Each participants functional dataset underwent standard pre-processing steps (Slice-scan time correction, three-dimensional motion correction, and temporal high-pass filtering. Each participants anatomical data underwent intensity inhomogeneity correction, ISO-voxel (1x1x1mm) transformation, followed by normalization to a standard Montreal Neurological Institute (MNI) brain template. Next, the preprocessed functional and anatomical data were co- registered. Initial and fine-tuning alignment were completed, and a volume time course information file was created for each participant.

Neurophysiological activity data were extracted from the Hippocampus. Additionally, we extracted data from the thalamus and from the Amygdala for reasons of comparison and validation. The BrainVoyager analyses software of-

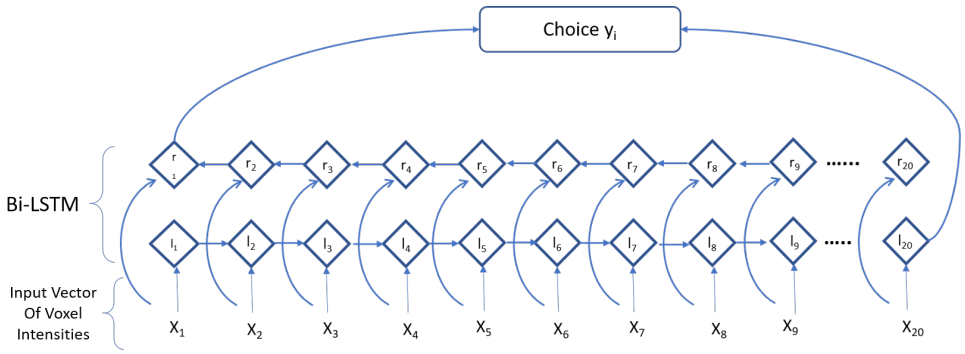

Figure 3: Shows the architecture of a bi-directional LSTM network modeled considering each choices made by the participant as one independent data entity. We input a vector of voxel intensities to the bi-directional LSTM with a sigmoid output layer.

fers a pre-defined volume of interest (VOI) files that map voxel coordinates to subcortical regions. Then, we made use of the NeuroElf module (http://neuroelf.net) and MATLAB to extract time course of intensity values from the volume time course file at every voxel specified in the VOI file.

Each trial, lasted for 20 seconds. The corresponding twenty volumes of intensity values were extracted and stored in comma-separated values (CSV) file. Each participant made ten choices, hence yielded ten comma-separated values files.

4 Support Vector Machine(SVM)

we submitted the data to a support vector machine(Chang and Lin, 2011), representing a useful technique for data classification (i.e., a non-probabilistic binary classifier). The standard support vector machine uses a linear decision boundary, given by $(\omega^T x_{new} + b)$, to classify new data objects. Objects lying on one side of the decision boundary are put into class $t_{new} = 1$ and objects on the other side into $t_{new} = -1$.

$$t_{new} = sign(\omega^T x_{new} + b)$$

Since we are dealing with time series data as input, we used the below approaches to convert the time series data to feature vectors:

- Average: We took the average of intensity values across time at each voxel. Our training data for each choice ended up having 12,910 features, one corresponding to every voxel.
- Variance: We took the variance of intensity values across time at each voxel. Our training data for each choice ended up having 12,910 features, one corresponding to every voxel.

Training set consists of instance-label pairs (x_i, y_i), $i = 1, 2, ...n$ where x_i is the vector of temporal voxel intensities corresponding to a particular choice and y_i belongs to $\{1, -1\}$ (1 if the participants chose high-variance choice and, -1 if the participants chose low-variance choice). Each choice is made by a participant are treated to be independent.

After performing Leave one out cross validation (LOOCV) on 46 subjects neuroimaging data results revealed average prediction accuracy of 57.6% for the Hippocampus region.

5 Long Short-Term Memory(LSTM)

An LSTM model is ideal choice for modeling fMRI data. Prior research has shown that LSTM models can significantly outperform established response models by accurately estimating long-term dependencies that drive haemodynamic responses(Gl and van Gerven, 2017).

5.1 Bi-LSTM: Choice-wise

We treat each choice made by the participant as an independent entity and train the LSTM. Out of 46 participants, we used 40 subjects data for training and 6 subjects data for testing. Our training data consisted of instance-label pairs ($[x_1$,x_2,x_3,...,$x_{20}]_i$, y_i), where x_i is a vector of intensity values at all voxels in the region of interest at time point t. y_i is -1,1, 1 if the participants chose a high-variance choice and, -1 if the participants chose low-variance choice). See Figure3 for Bi-LSTM choice-wise network architecture.

We trained our model using Stochastic Gradient Descent (SGD) algorithm with a learning rate of 0.05 and gradient clipping of 5. SGD performed better than Adagrad, RMSProp, and Adam. We set batch size as 1. LSTM is bi-directional and has one layer whose dimensions are set to 100. We experimented with different dropout rates and 0.4

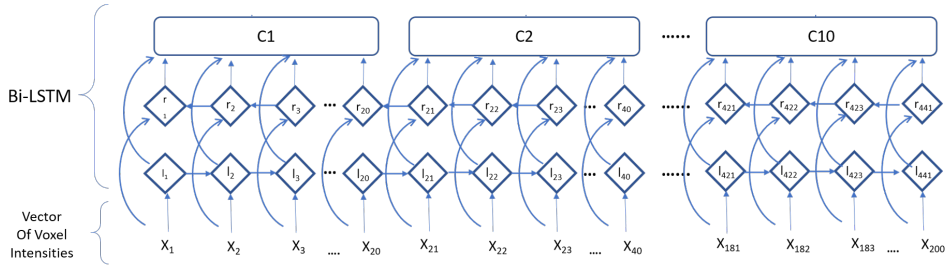

Figure 4: Shows the architecture of a bi-directional LSTM network modeled by considering all the choices made by the participant as data entity. We input a vector of voxel intensities to the bi-directional LSTM with a sigmoid output layer.

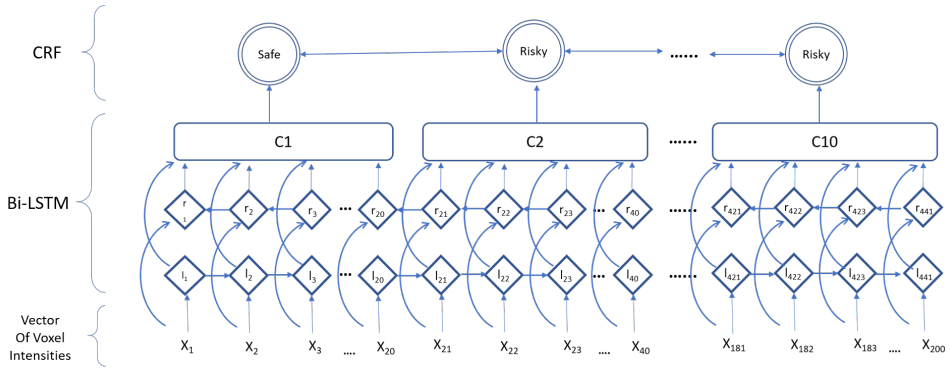

Figure 5: Shows the architecture of a bi-directional LSTM-CRF network. CRF mounted on top of the LSTM captures label dependencies.

gave the best performance. We used early stopping by monitoring the accuracy.

5.2 Bi-LSTM: Subject-wise

We consider one participant as one data entity. We feed the complete volume time course file consisting of 200 volumes (20 volumes per trial) as input to the Bi-LSTM and predict the sequence of choices made by the participant as output. Our training data consists of instance-label pairs $([x_1,x_2,x_3,...,x_{200}]_i, [y_1,y_2,y_3,...,y_{10}]_i)$. For participant i, we have x_k, where $1 < k < 200$ (total volumes) is the vector of intensity values at all the voxels in the region of interest at time point t.and y_m where $1 < m < 10$ is a vector of 10 choice labels made by the participant, 1 if the participants chose a high-variance choice and, -1 if the participants chose low-variance choice). See Figure 4 for Bi-LSTM subject-wise network architecture.

5.3 Error Analysis

Participants in the study preferred the high-variance options more often than the low-variance options (57 to 43). As we can see from the confusion matrix, the percentage of safe choices being classified as risky is higher than risky choices being classified as safe. The order in which these choices were presented was kept the same for all participants. This may have some contribution to the selection bias towards risky choices.

	Risky	Safe
Risky	22	7
Safe	12	19

Table 1: Table shows the confusion matrix for classification using the Bi-LSTM subject-wise model. Rows represent true values and columns represent classifier predictions

6 LSTM-CRF

LSTMs model sequences but don't capture dependencies between labels. In the Bi-LSTM subject-wise model, when we predict the choices made by a participant as a sequence, it is important to understand the dependencies that exist within the labels. Therefore, instead of predicting choices independently, we model them jointly using a conditional random field (CRF). CRFs excel at capturing these dependencies. (Lample et al., 2016) We take inspiration from Named Entity Recognition (NER) task in language processing and apply a LSTM-CRF model to fMRI data. We extend the Bi-LSTM subject-wise model to include a CRF at the top most layer. See Figure 5 for LSTM-CRF architecture,

7 Results

Model	Accuracy
SVM (Linear, Average)	57.60
Bi-LSTM choice-wise	68.04
Bi-LSTM subject-wise	69.13
LSTM-CRF	**77.82**

Table 2: Table shows the prediction accuracies for SVM and different LSTM architectures. The region under consideration is Left-Hippocampus and Leave One Out Cross Validation (LOOCV) is used to evaluate the models. SVM uses linear kernel and average voxel intensities as feature vectors. We used SGD with learning rate as 0.05 and gradient clipping at 5.0 to optimize all Bi-LSTM and LSTM-CRF models. We set the batch size as 1, dropout rate 0.4, Early Stopping (patience=3 epochs, min delta=0.1, monitor=accuracy)

As you can see from Table 2, LSTMs outperform SVM significantly. SVM is using average intensity across time as feature and we are losing information in that process. The difference in prediction accuracy by modeling the choices independently and jointly (choice-wise and subject-wise) is quite small. However, we notice a significant jump in prediction accuracy by using a LSTM-CRF. In the confusion matrix (Table 3) we can see a decrease in the percentage of safe choices being classified as risky.

	Risky	Safe
Risky	24	5
Safe	8	23

Table 3: Table shows the confusion matrix for classification using LSTM-CRF model. Rows represent true values and columns represent classifier predictions

8 Conclusion

fMRI data is an indirect measure of neural activity, has low signal to noise ratio, high-dimensional and includes an intrinsic delay (Haemodynamic Response Function) which makes it hard to classify. We are able to predict consumers choices using fMRI data with accuracies exceeding chance percentage. Understanding the dependencies on how consumers transition from making risky and safe choices by modelling a CRF, helps improve the accuracy considerably. While these results only allow cautious interpretation regarding the involvement of explicit memory, they nonetheless pave the way for future studies that could hone the experimental design to obtain higher prediction accuracies.

References

Chih-Chung Chang and Chih-Jen Lin. 2011. LIBSVM: A library for support vector machines. *ACM Transactions on Intelligent Systems and Technology*, 2:27:1–27:27. Software available at http://www.csie.ntu.edu.tw/~cjlin/libsvm.

Nathawani Dhruv, Sharma Tushar, and Yang Yang. 2016. Neuroscience meets deep learning. Retrieved from http://www.andrew.cmu.edu/user/dnathawa/documents/10-701Dhruv.pdf.

Umut Gl and Marcel A. J. van Gerven. 2017. Modeling the dynamics of human brain activity with recurrent neural networks. *Frontiers in Computational Neuroscience*, 11:7.

J.D. Haynes and G. Rees. 2005. Predicting the stream of consciousness from activity in human visualcortex. *Science Direct*, 15:1301–1307.

Dongling Huang and Lan Luo. 2016. Consumer preference elicitation of complex products using fuzzy support vector machine active learning. *Special Issue of Marketing Science on Big Data Integrating Marketing, Statistics, and Computer Science*, 35:341–537.

D. Kahneman and A. Tversky. 1979. Prospect theory: An analysis of decision under risk. *Econometria*, 47(2):263–291.

D. Kahneman and A. Tversky. 1992. Advances in prospect theory: Cumulative representation of uncertainty. *Journal of Risk and Uncertainty*, 5(4):297–323.

E. R. Kandel. 2007. *In search of memory: The emergence of a new science of mind*. WW Norton and Company.

E.R. Kandel. 2001. The molecular biology of memory storage: A dialogue between genes and synapses. *Science*, 294(5544):1030–1038.

A. Norman Kenneth, M. Polyn Sean, J. Detre Greg, and V. Haxby James. 2006. Beyond mind-reading: Multi-voxel pattern analysis of fmri data. *Trends in Cognitive Scince*, 10(9):424–430.

Guillaume Lample, Miguel Ballesteros, Sandeep Subramanian, Kazuya Kawakami, and Chris Dyer. 2016. Neural architectures for named entity recognition. *CoRR*, abs/1603.01360.

Jolie M. Martin, Martin Reimann, and Michael I. Norton. 2016. Experience theory, or how desserts are like losses. *Journal of Experimental Psychology*, 145(11):1460–1472.

Sean M. Polyn, Vaidehi Natu, Jonathan D. Cohen, and Kenneth A. Norman. 2005. Category-specific cortical activity precedes retrieval during memory search. *Science*, 310:1963–1966.

M. Rabin and R.H. Thaler. 2001. Anomalies: Risk aversion. *Journal of Economic Perspectives*, 15(1):219–232.

Goebel Rainer, Esposito Fabrizio, and Elia Formisano. 2006. Analysis of functional image analysis contest (fiac) data with brain voyager qx. *Human Brain Mapping*, 27:392–401.

M. Reimann, O. Schilke, B. Weber, C. Neuhaus, and J. Zaichkowsky. 2011. Functional magnetic resonance imaging in consumer research: A review and application. *Psychology and Marketing*, 28(6):608–637.

L.R. Squire and S. Zola-Morgan. 1991. The medial temporal lobe memory system. *Science*, 253(5026):1380–1386.

Nur Farahana Mohd Suhaimi, Zaw Zaw Hitke, and Nahrul Khair Alang Md Rashid. 2015. Studies on classification of fmri data using deep learning. *ARPN Journal of Engineering and Applied Sciences*, 10:9748–9752.

APPENDIX

Experiment Design

Participants: Forty-six adult volunteers were recruited from the subject pool of a large university, invited to the functional neuroimaging facility, and were engaged in a behavioral decision-making task in which they had to repeatedly choose between two music songs (i.e.,two experiences) or two monetary gambles. While participants were engaged in the task, their neurophysiological responses were recorded.

Procedures: Upon arrival at the functional neuroimaging facility, participants were asked to provide written informed consent to a protocol approved by an institutional review board. Before entering the functional neuroimaging scanner (i.e., a Siemens Skyra 3 Tesla scanner), participants were engaged in a practice version of the behavioral task. Also before being positioned inside the scanner, participants indicated their most preferred music genre from a list of 22 genres (e.g., classical, hip-hop, jazz, rock). In accordance with Prospect Theory to put the participants into a state of monetary gains, they were provided with a $25 cash endowment and were asked to put the bills in their pocket. We aimed to make the subsequent monetary choices incentive-compatible in the sense that participants made real monetary choices from their own endowment. Next, participants were told that we would like them to make monetary choices in different games of chance, and that during these games, they might either lose some or all of their $25 stake, retain it, or increase it. Next, following prior research (Martin et al., 2016), participants received the instructions on how to interpret their experiential choices.

Participants were then guided to the fMRI scanner, placed horizontally on a bed, and moved inside the scanner. The behavioral task was projected onto a mirror that was placed right above participants eyes. Participants were able to provide all behavioral responses via a standard button box. For a more detailed description of standard fMRI experimental procedures see the primer by (Reimann et al., 2011).

Once comfortably situated inside the scanner, participants were asked to make five monetary choices and five experiential choices in pseudo-random order. They were prompted to evaluate the two choice options, which always had a low-variance choice (risk-averse option) and a high-

variance choice (risk-seeking option). The high- and low-variance options were identical in their expected value set to zero. Each of these ten product choices followed the trial structure. In particular, participants were initially shown a fixation cross to focus their attention on the center of the screen (fixation phase, timed between two and four seconds long). Participants were then provided a prompt telling them whether to expect two song options or two monetary gamble options (trial introduction phase, timed two seconds long). Next, participants were provided with the actual two options, a low-variance choice and a high-variance choice and given ample time to interpret the given options (risk judgment phase, timed twelve seconds long). Participants were then prompted to choose one option from the choice set (choice phase, timed two seconds long), followed by a brief confirmation of their choice (choice confirmation phase, timed two seconds long) before the next trial started.

In summary, the repeated-measures design yielded a dataset containing 460 individual choices (46 subjects 10 choices). Because the behavioral task is precisely timed, we were able to analyze the brain activity during the time frame in which participants judged the experiential or monetary options, followed by participants actual choice response. We were thus able to test our prediction that making choices on experiences will result in greater neurophysiological activity (i.e., greater blood-oxygen-level-dependent responses) in the medial temporal lobe compared to making choices on money, possibly because participants are using extreme reference points stored in explicit memory to a greater extent under experiential choices than monetary choices. In summary, the present experiment yielded both behavioral choice data as well as functional neuroimaging data.

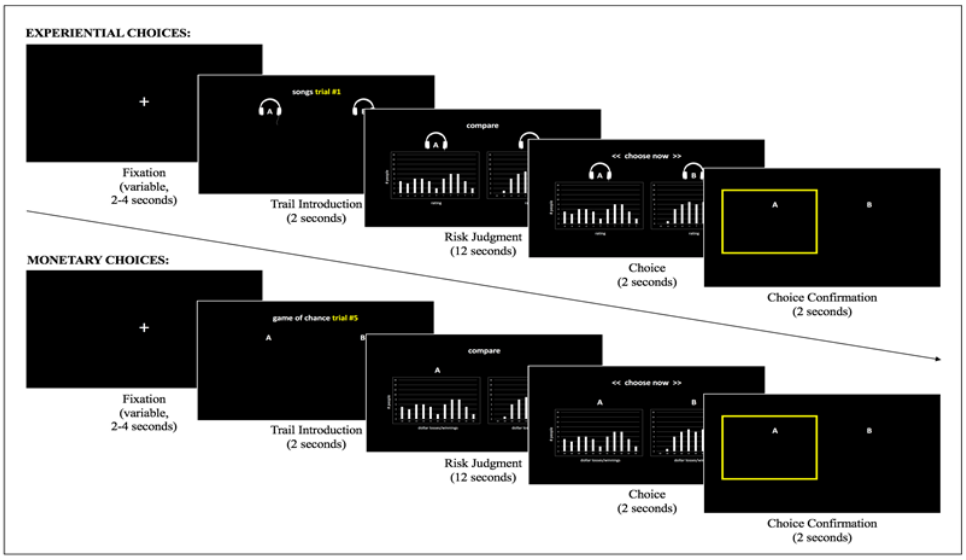

Figure 6: Shows a series of slides viewed by the participant in each trial. There were 10 trial s in total, 5 experiential and 5 monetary, which were presented to the participant in pseudo-random order. The order remained the same for all subjects. The fixation phase varied in length for each trial. Length of all the other phases remained the same throughout the experiment.

In addition to choices on games of chance, today's task is also designed to find out how you make choices between different music songs based on the **actual ratings other people** have given.

You will make choices on different music songs, for this music genre:

Today, you will choose between 5 different sets of songs and **get to take home your 5 chosen ones**.

For each music song, we will show you a chart where the heights of the bars above a number indicate the number of people who gave the song that rating.

Please read the following example carefully:

57 UA students rated different songs on a scale from -5 to +5, -5 being the worst, +5 being the best.

In this chart, five people gave the song a rating of -5, twelve people gave the song a rating of -5, and so on. Please study this chart for a minute:

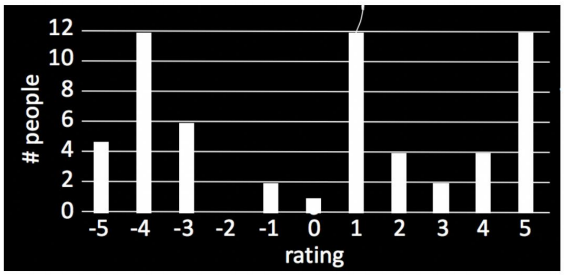

Thank you! Please hand the package over to the researcher.

Figure 7: Instructions to interpret experiential choice options. These instructions were provided to the participants before they were placed inside the scanner.

To make these choices, we will need to introduce you to the following charts:

Today's task is designed to find out how you make choices between different games of chance based on the **actual losses/winnings** of other people.

For each game of chance, we will show you a chart where the heights of the bars above a specific loss or winning indicate the number of people who lost or won, respectively.

Please read the following example carefully:

57 UA students participated in different games of chance with outcomes from -$5 to +$5, -$5 being the worst, +$5 being the best.

In this chart, five people lost $5, twelve people lost $4, and so on. Please study this chart for a minute:

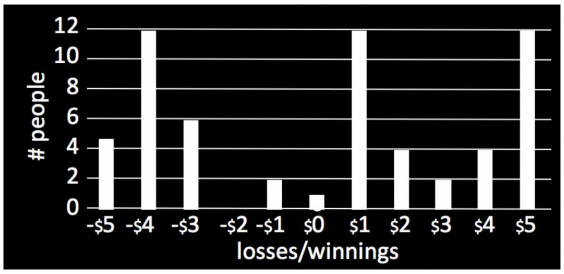

Please turn the page for more information.

Figure 8: Instructions to interpret gambling choice options. These instructions were provided to the participants before they were placed inside the scanner.